

# Shear yielding and shear jamming of dense hard sphere glasses

Pierfrancesco Urbani<sup>1</sup> and Francesco Zamponi<sup>2</sup>

<sup>1</sup>*Institut de physique théorique, Université Paris Saclay, CNRS, CEA, F-91191 Gif-sur-Yvette*

<sup>2</sup>*Laboratoire de Physique Théorique, ENS & PSL Univeristy,  
UPMC & Sorbonne Universités, UMR 8549 CNRS, 75005 Paris, France*

We investigate the response of dense hard sphere glasses to a shear strain, in a wide range of pressures ranging from the glass transition to the infinite-pressure jamming point. The phase diagram in the density-shear strain plane is calculated analytically using the mean field infinite dimensional solution. We find that just above the glass transition, the glass generically yields at a finite shear strain. The yielding transition, in the mean field picture, is a spinodal point in presence of disorder. At higher densities, instead, we find that the glass generically jams at a finite shear strain: the jamming transition prevents yielding. The shear yielding and shear jamming lines merge in a critical point, close to which the system yields at extremely large shear stress. Around this point, a highly non-trivial yielding dynamics characterized by system-spanning disordered fractures is expected.

*Introduction* – The response of glasses to a shear strain is extremely complex and has always been the subject of much interest, for fundamental and technological reasons [1–5]. While at small enough strains the solid responds elastically, at moderate strains the response is characterized by small intermittent drops of the shear stress. At larger strains, the stress drops abruptly when the glass yields. Above yielding, the stress remains approximately constant upon increasing strain, and the system flows [4, 5]. For soft interaction potentials, it has been established that both low-stress intermittency and large-stress flow are due to “plastic” events at which small regions of the material – called “shear transformation zones” – fail under stress [2, 4, 6, 7]. The energy relaxed by the failure is propagated elastically through the system, leading to failure in other regions. The stress-strain curves can be well described by elasto-plastic models, that describe mesoscopically the coupling between failing regions [8–10], and the shear transformation zones have been identified quite precisely in numerical simulations [6, 7].

The situation is quite different for dense hard sphere glasses, that are good models of colloidal and granular glasses. These solids, due to the hard sphere constraints, are characterized by a critical “random close packing” or “jamming” density at which a rigid isostatic network of particle contacts emerges, inducing a divergence of the pressure [11–13]. Around the jamming point, due to the emergent contact network, perturbing a particle leads to a macroscopic rearrangement of the whole solid [14–16]: continuum elasticity breaks down [17–20] and solid dynamics is characterized by system-spanning avalanches during which the system relaxes along strongly delocalized soft modes [20–22]. Clearly, in this regime the “shear transformation zone” picture becomes inappropriate.

The aim of this Letter is to characterize the response of a dense hard sphere glass to a shear strain, all the way from the glass transition to the jamming regime. We find that at lower densities, slightly above the glass tran-

sition, the hard sphere glass responds in a way similar to soft particle glasses: an elastic regime is followed by an intermittent regime before the system yields (“shear yielding”). At larger densities, close to jamming, the situation is radically different. Before yielding, a jamming transition happens due to shear: at the transition a rigid network of contacts is formed and the pressure diverges (“shear jamming”). The shear jamming transition is in the same universality class of the jamming transition at zero shear [23, 24], and it is characterised by non-trivial critical exponents that appear in the interparticle force and gap distributions [14, 25, 26]. Most importantly, the shear yielding and shear jamming lines merge in a critical point. Around this point, because the system yields at extremely large (diverging) pressure and shear stress, in a regime of incipient jamming, we expect a highly non-trivial yielding dynamics, characterized by system-spanning disordered fractures.

*Glass preparation protocol* – We consider a system of  $N$  identical  $d$ -dimensional hard spheres, in the thermodynamic limit at constant number density  $\rho$  and volume fraction  $\varphi$ . We consider the limit  $d \rightarrow \infty$ , with constant  $\hat{\varphi} = 2^d \varphi / d$ , in which the liquid and glass properties can be computed exactly within the mean field Random First Order Transition scenario [27, 28]. For hard spheres, the infinite dimensional limit usually provides qualitatively good predictions for the phase diagram of low-dimensional systems [28], especially around jamming [25], and finite-dimensional effects can be studied through numerical simulations [26, 29]. Also, for  $d > 3$  polydispersity is not needed, as monodisperse hard spheres are a very good glass-forming system [30, 31].

During a slow cooling of a liquid, the relaxation time scale  $\tau_\alpha(\hat{\varphi})$  becomes extremely large around the Mode-Coupling density  $\hat{\varphi}_d$ , but one can still equilibrate up to quite larger values of  $\hat{\varphi}$ , either by brute force [34] or by means of smart numerical algorithms [35–38] and smart experimental protocols [39]. Once equilibration at some  $\hat{\varphi}_g > \hat{\varphi}_d$  has been achieved, one can focus on time scales

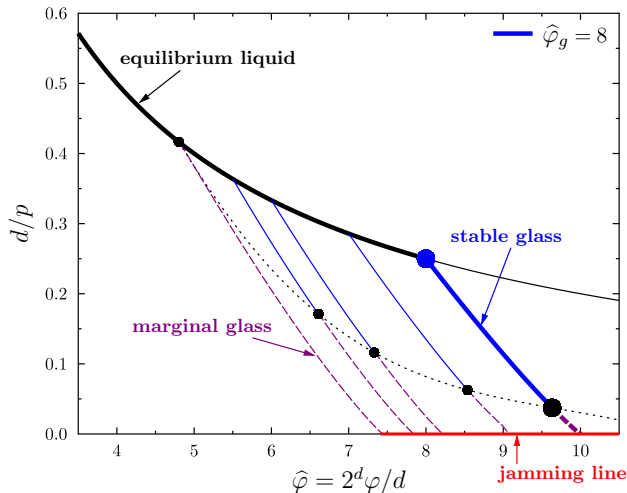


FIG. 1. Inverse reduced pressure  $d/p$  versus packing fraction  $\hat{\varphi} = 2^d \varphi/d$  (both scaled to remain finite for  $d \rightarrow \infty$ ) during a slow compression [32, 33]. The liquid EOS is  $d/p = 2/\hat{\varphi}$ . The dynamical transition  $\hat{\varphi}_d$  is marked by a black dot. We focus on a liquid slowly compressed up to  $\hat{\varphi}_g = 8$  (blue full circle). From that point on, the system is followed in a restricted equilibrium confined to the glass state (full blue line). At high pressure, the glass state becomes marginally stable. Jamming is reached around  $\hat{\varphi}_j \approx 10$ . The thick lines indicate the specific glass we follow in this paper. Other glasses corresponding to different  $\hat{\varphi}_g$  (different compression rates) are plotted with thinner lines.

$\tau_{\text{exp}} \ll \tau_{\alpha}(\hat{\varphi}_g)$ , in such a way that the system remains confined in the glass state selected in equilibrium at  $\hat{\varphi}_g$ .

In the mean field limit  $d \rightarrow \infty$ , the liquid relaxation time diverges above  $\hat{\varphi}_d$ , and the dynamics is completely arrested [27, 40, 41]. The separation of time scales thus becomes very sharp as  $\tau_{\text{exp}} \ll \tau_{\alpha}(\hat{\varphi}_g) \rightarrow \infty$ . The “state following” formalism is designed to describe this regime [42–44], in which a typical equilibrium configuration selects a long-lived glass basin which is then adiabatically followed upon increasing the density  $\hat{\varphi} \geq \hat{\varphi}_g$  and applying a shear strain  $\gamma$  [28, 32, 33]. In particular, the method gives the reduced pressure  $p = \beta P/\rho$  and shear stress  $\sigma = \beta \Sigma$  of the glass.

The pressure-density equation of state in absence of shear has been studied in [32, 33] (Fig. 1). We focus on a liquid compression that remains in equilibrium until  $\hat{\varphi}_g = 8 > \hat{\varphi}_d \approx 4.8$  (but our results are independent on this choice), and we follow the corresponding glass in a restricted equilibrium. This glass undergoes a Gardner phase transition to a marginally stable state [25, 28, 32, 33], and then jams at a density  $\hat{\varphi}_j \approx 10$ . The phase diagram of Fig. 1 qualitatively agrees with  $3d$  numerical simulations [38].

**Stress-strain curves** – The glass prepared at  $\hat{\varphi}_g$  is first adiabatically compressed to  $\hat{\varphi} > \hat{\varphi}_g$ . Then, a shear strain  $\gamma$  is applied and we compute the stress  $\sigma$ . At the replica

symmetric level [45], the glass free energy  $f_g(\gamma, \hat{\varphi}; \Delta, \Delta_r)$  can be exactly computed in  $d \rightarrow \infty$  as a function of two order parameters [32]:  $\Delta$  is the mean square displacement (MSD) in the glass state at  $(\hat{\varphi}, \gamma)$ , and  $\Delta_r$  is the relative MSD of a typical glass configuration and the equilibrium configuration at  $\hat{\varphi}_g$ . Both are obtained by setting the derivatives of  $f_g$  to zero. Once  $\Delta, \Delta_r$  are determined, the reduced pressure  $p$  and stress  $\sigma$  are derivatives of  $f_g$  with respect to  $\hat{\varphi}$  and  $\gamma$ , respectively.

All the four quantities  $p$ ,  $\sigma$ ,  $\Delta$  and  $\Delta_r$  are reported in Fig. 2 as functions of  $\gamma$  for several values of  $\hat{\varphi}$ . We observe a different behavior at lower densities close to  $\hat{\varphi}_g = 8$  and at higher densities close to  $\hat{\varphi}_j \approx 10$ . For lower  $\hat{\varphi}$ , there is first a linear elastic regime  $\sigma \sim \mu\gamma$ , followed by a stress overshoot before the system finally yields at  $\gamma_y(\hat{\varphi})$ . At yielding, stress, pressure,  $\Delta$  and  $\Delta_r$  all remain finite, but they all display a square-root singularity, e.g.  $p - p_y \propto \sqrt{\gamma_y - \gamma}$ . This happens because in mean field, yielding is akin to a spinodal: the solution of the stationarity equations for  $\Delta, \Delta_r$  merges with another unphysical solution and disappears in a bifurcation-like manner. This is related to the vanishing of a *longitudinal mode*  $\lambda_L \propto d^2 f_g / d\Delta_r^2$ . It also implies that there is a diverging susceptibility at  $\gamma_y(\hat{\varphi})$ , related to the fluctuations of  $\Delta_r$ :  $\chi_L \sim \langle \Delta_r^2 \rangle - \langle \Delta_r \rangle^2 \propto 1/\lambda_L$ . For higher  $\hat{\varphi}$ , instead, we observe that pressure and stress increase fast and both diverge at a shear jamming point  $\gamma_j(\hat{\varphi})$ , where  $\Delta \rightarrow 0$  and  $\Delta_r$  remain finite.

**Phase diagram** – In Fig. 3 the shear yielding line  $\gamma_y(\hat{\varphi})$  and the shear jamming line  $\gamma_j(\hat{\varphi})$  are reported in the  $(\hat{\varphi}, \gamma)$  plane for  $\hat{\varphi}_g = 8$ . We observe a re-entrant shear jamming line, moving to lower densities for increasing  $\gamma$ . The shear yielding line  $\gamma_y$  decreases upon increasing  $\hat{\varphi}$ . It is possible to show analytically that the two lines merge at a critical point  $(\hat{\varphi}_c, \gamma_c)$ , at which the system is both jammed (because  $\Delta = 0$ ,  $p = \infty$ ,  $\sigma = \infty$ ) and yielding, because the longitudinal mode vanishes indicating an instability of  $\Delta_r$  (which remains finite at the critical point, but has infinite derivative).

**Marginal stability** – As previously found in [32, 33], the replica symmetric solution used to compute the results of Fig. 2 becomes unstable in a region of the phase diagram delimited by the *Gardner transition line*  $\gamma_G(\hat{\varphi})$ . Beyond this line, the order parameter  $\Delta$  becomes a function  $\Delta(x)$  defined for  $x \in [0, 1]$  and the glass free energy is a functional  $f_g[\gamma, \hat{\varphi}; \Delta(x), \Delta_r]$ . The resulting *full replica symmetry breaking* solution [45] is characterized by marginal stability: one of the derivatives of the free energy (the *replicon* mode) is identically vanishing in the marginally stable phase, leading to a diverging susceptibility and the breakdown of standard elasticity [19, 28]. The function  $\Delta(x)$  and  $\Delta_r$  are determined by setting the (functional) derivatives of  $f_g$  to zero. Although we did not solve the resulting equations numerically (see [33] for a computation of the stress-strain curves at  $\hat{\varphi}_g$ ), the phase diagram remains qualitatively similar to Fig. 3.

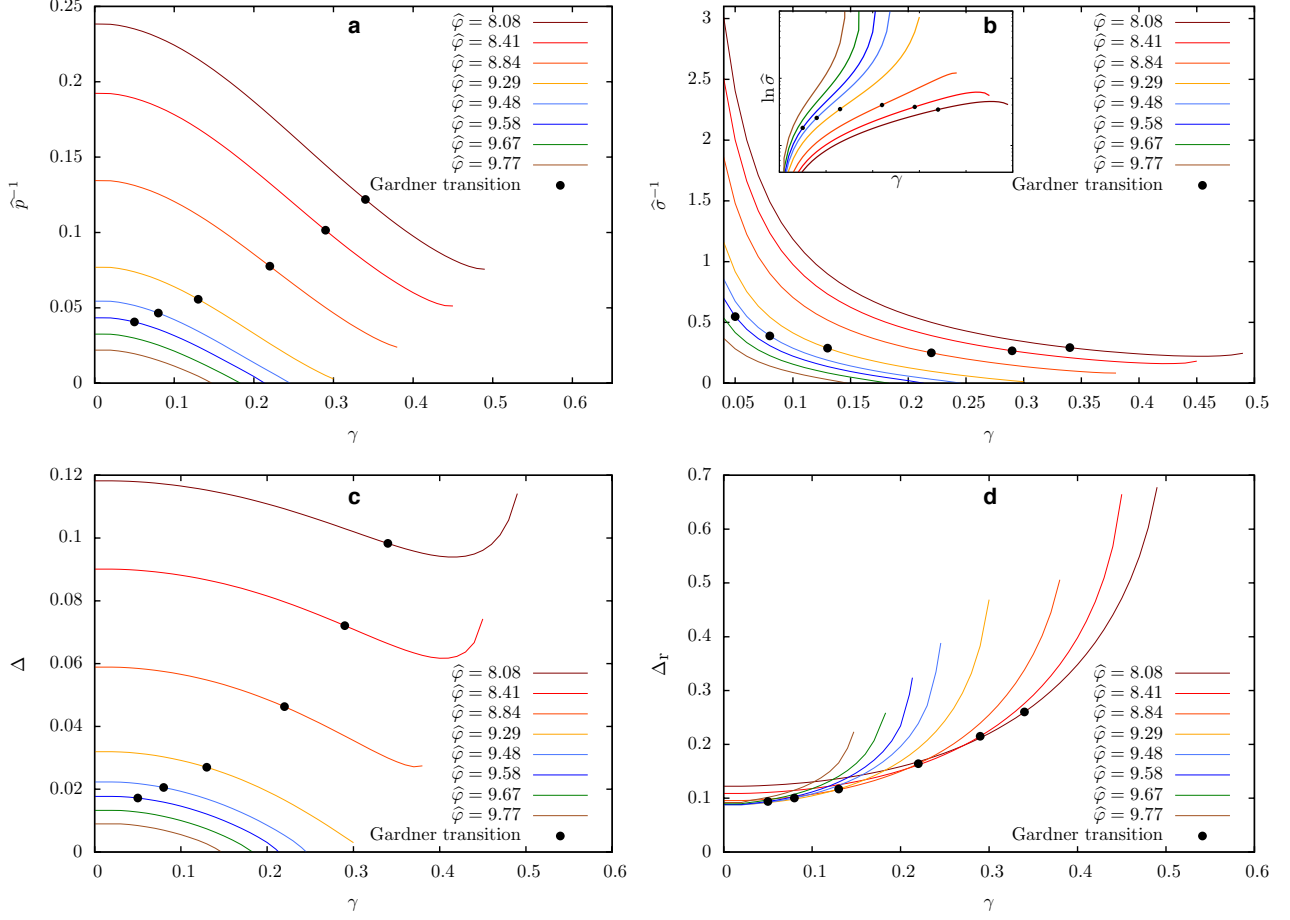


FIG. 2. Applying adiabatically a shear strain  $\gamma$  on a glass prepared at equilibrium at  $\hat{\varphi}_g = 8$  and adiabatically compressed to  $\hat{\varphi} \in [\hat{\varphi}_g, \hat{\varphi}_j]$ . The black dots along the lines represent the Gardner transition. **(a)** Inverse reduced pressure  $d/p \equiv \hat{p}^{-1}$  vs  $\gamma$ . At lower  $\hat{\varphi}$ , the pressure is finite until the system yields at  $\gamma_y(\hat{\varphi})$ . At higher density, the pressure diverges at the shear jamming point  $\gamma_j(\hat{\varphi})$ . **(b)** Inverse of the reduced shear stress  $\hat{\sigma}^{-1} \equiv d/\sigma$  vs  $\gamma$ . The behavior is very similar to the pressure. At lower  $\hat{\varphi}$ , the stress overshoots before yielding. At higher  $\hat{\varphi}$ , the stress diverges at  $\gamma_j$  without any overshoot. The inset shows the behavior of  $\ln \hat{\sigma}$  vs  $\gamma$ . **(c)** The glass MSD  $\Delta$  vs  $\gamma$ . At lower  $\hat{\varphi}$ ,  $\Delta$  remains finite at yielding. At higher  $\hat{\varphi}$ ,  $\Delta$  vanishes at shear jamming. **(d)** The MSD  $\Delta_r$  between the initial equilibrium configuration at  $\hat{\varphi}_g$  and the one at  $(\hat{\varphi}, \gamma)$ . At lower  $\hat{\varphi}$ ,  $\Delta_r$  remains finite and displays a square-root singularity at yielding, such that  $d\Delta_r/d\gamma \rightarrow \infty$  for  $\gamma \rightarrow \gamma_y$ . At higher density,  $\Delta_r$  remains finite at shear jamming with no singularity.

Indeed, we can show analytically that *(i)* shear jamming is characterized by the vanishing of  $\Delta(1)$ , the self MSD of the glass states, which induces a divergence of pressure  $p$  and stress  $\sigma$ . On the shear jamming line, the critical properties are the same of the jamming point at zero strain [25]: the inter-particle force and gap distributions display power-law behavior, with non-trivial exponents that are constant along the shear jamming line. *(ii)* Shear yielding is still characterized by the vanishing of  $\lambda_L \propto d^2 f_g / d\Delta_r^2$ , which induces a divergence of the fluctuations of  $\Delta_r$ . However, the critical properties on the shear yielding line remain to be understood. *(iii)* The two lines merge at a critical point where both  $\Delta(1) = 0$  and  $\lambda_L = 0$ .

*Comparison with numerics and experiments* – Many experimental and numerical works have studied both shear yielding and shear jamming. In particular, simulations of athermal systems [24, 46–50] and experiments on granular materials [51–53] found a re-entrant shear jamming line. However, for athermal systems, the re-entrance is a finite size effect and disappears when  $N \rightarrow \infty$  [24]. This is expected from the theory because for hard spheres, when  $T \rightarrow 0$ , both the pressure  $P = Tp$  and the stress  $\Sigma = T\sigma$  vanish, so there cannot be any shear jamming at  $T = 0$ . While athermal systems ( $T = 0$ ) below jamming are fluid and flow for any  $\gamma$ , for thermal hard spheres (any  $T > 0$ ) entropic forces stabilize the solid phase in the region delimited by the

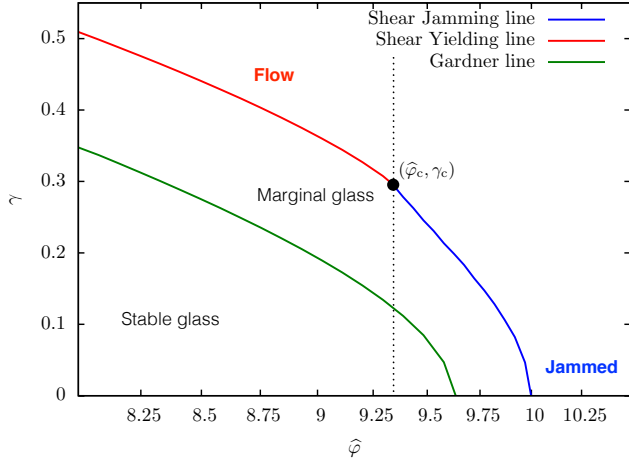


FIG. 3. Phase diagram of the glass prepared in equilibrium at  $\hat{\varphi}_g = 8$ , and followed adiabatically at density  $\hat{\varphi} > \hat{\varphi}_g$  and shear strain  $\gamma$ . The shear jamming line  $\gamma_j(\hat{\varphi})$  and the shear yielding line  $\gamma_y(\hat{\varphi})$  are plotted. The two lines merge at a critical point  $(\hat{\varphi}_c, \gamma_c)$ . At this special point, yielding happens at infinite pressure/strain. For  $\hat{\varphi} \lesssim \hat{\varphi}_c$ , yielding happens at  $\gamma \sim \gamma_c$  with extremely large pressure/strain.

shear yielding and shear jamming lines in Fig. 3. Granular materials, due to tapping, could be equivalent to thermal systems and display a re-entrance that persists for  $N \rightarrow \infty$ , but a finite-size study has not been performed in this case [51–53]. Also, the results of [54, 55] on shear yielding support the idea that this transition is similar to a spinodal point in presence of disorder. A more direct comparison can be made between our theory and very recent simulations of thermal hard spheres under shear [56]. Our predictions are qualitatively compatible with these numerical results. However, none of these studies has investigated the coalescence of the shear yielding and shear jamming lines at  $(\varphi_c, \gamma_c)$ , and the plastic dynamics around the critical point, which is the most interesting result of this work.

Although our results are derived in a mean field setting, we expect that they are quantitatively accurate to describe the jamming criticality in finite dimensions, as it is the case for  $\gamma = 0$  [25]. Instead, the mean field theory of the yielding transition must be corrected in finite dimensions [57, 58]. However, at the critical point  $(\hat{\varphi}_c, \gamma_c)$ , we expect that the system sizes where finite  $d$  corrections become important diverge, so that the mean field theory of the yielding transition can likely become exact close to  $(\hat{\varphi}_c, \gamma_c)$ . We underline that in standard models of spinodal transition with disorder [57, 58], this never happens and the spinodal transition is not described by mean field in any dimension.

**Conclusions** – We investigated the phase diagram of a dense hard sphere glass, prepared in equilibrium at  $\hat{\varphi}_g > \hat{\varphi}_d$ , and followed adiabatically to density  $\hat{\varphi}$  and

shear strain  $\gamma$ . The phase diagram in the  $(\hat{\varphi}, \gamma)$  plane (Fig. 3) generically displays a shear yielding line when  $\hat{\varphi} \gtrsim \hat{\varphi}_g$ , and a shear jamming line when  $\hat{\varphi} \lesssim \hat{\varphi}_j$ . The two lines merge at a critical point, around which the system yields at extremely large pressure and shear stress. The plastic dynamics around this critical point is expected to be strongly different from the one of soft glasses. Its analytical and numerical investigation is a very interesting subject for future work. The shear jamming line has the same critical properties of the isotropic jamming transition [23–25]. The critical properties of the shear yielding line have not yet been investigated, because this line falls in a region where the glass is marginally stable and, at the mean field level, a full replica symmetry breaking scheme is needed. Its characterization is a very difficult task but it is certainly another very important line for future research. Systematic numerical investigation of the phase diagram in Fig. 3, following [56], will be of great help to fully understand the interplay of yielding and jamming in amorphous solids.

**Acknowledgments** – We thank M. Baity Jesi, G. Biroli, O. Dauchot, Y. Jin, S. Sastry, H. Yoshino, E. De Giuli and M. Wyart for many useful discussions. This work was supported by a grant from the Simons Foundation (#454955, Francesco Zamponi).

- 
- [1] A. Argon and H. Kuo, *Materials science and Engineering* **39**, 101 (1979).
  - [2] M. Falk and J. Langer, *Physical Review E* **57**, 7192 (1998).
  - [3] P. Schall, D. A. Weitz, and F. Spaepen, *Science* **318**, 1895 (2007).
  - [4] J.-L. Barrat and A. Lemaître, in *Dynamical heterogeneities in glasses, colloids, and granular media*, edited by L. Berthier, G. Biroli, J.-P. Bouchaud, L. Cipelletti, and W. van Saarloos (Oxford University Press, 2011).
  - [5] D. Rodney, A. Tanguy, and D. Vandembroucq, *Modelling and Simulation in Materials Science and Engineering* **19**, 083001 (2011).
  - [6] F. Puosi, J. Rottler, and J.-L. Barrat, *Phys. Rev. E* **94**, 032604 (2016).
  - [7] A. K. Dubey, H. G. E. Hentschel, I. Procaccia, and M. Singh, [arXiv:1604.04088](https://arxiv.org/abs/1604.04088) (2016).
  - [8] P. Sollich, F. Lequeux, P. Hébraud, and M. E. Cates, *Physical review letters* **78**, 2020 (1997).
  - [9] P. Hébraud and F. Lequeux, *Physical review letters* **81**, 2934 (1998).
  - [10] E. Agoritsas, E. Bertin, K. Martens, and J.-L. Barrat, *The European Physical Journal E* **38**, 1 (2015).
  - [11] C. S. O’Hern, S. A. Langer, A. J. Liu, and S. R. Nagel, *Phys. Rev. Lett.* **88**, 075507 (2002).
  - [12] G. Parisi and F. Zamponi, *Rev. Mod. Phys.* **82**, 789 (2010).
  - [13] S. Torquato and F. H. Stillinger, *Rev. Mod. Phys.* **82**, 2633 (2010).
  - [14] M. Wyart, *Phys. Rev. Lett.* **109**, 125502 (2012).

- [15] E. Lerner, G. During, and M. Wyart, *Soft Matter* **9**, 8252 (2013).
- [16] E. DeGiuli, E. Lerner, C. Brito, and M. Wyart, *Proceedings of the National Academy of Sciences* **111**, 17054 (2014).
- [17] G. Combe and J.-N. Roux, *Physical Review Letters* **85**, 3628 (2000).
- [18] E. Lerner, E. DeGiuli, G. Düring, and M. Wyart, *Soft Matter* **10**, 5085 (2014).
- [19] G. Biroli and P. Urbani, *Nature Physics* (2016).
- [20] S. Franz and S. Spigler, [arXiv:1608.01265](#) (2016).
- [21] C. Brito and M. Wyart, *Europhysics Letters (EPL)* **76**, 149 (2006).
- [22] C. Brito and M. Wyart, *The Journal of Chemical Physics* **131**, 024504 (2009).
- [23] E. Lerner, G. Düring, and M. Wyart, *EPL (Europhysics Letters)* **99**, 58003 (2012).
- [24] M. Baity-Jesi, C. P. Goodrich, A. J. Liu, S. R. Nagel, and J. P. Sethna, [arXiv:1609.00280](#) (2016).
- [25] P. Charbonneau, J. Kurchan, G. Parisi, P. Urbani, and F. Zamponi, *Nature Communications* **5**, 3725 (2014).
- [26] P. Charbonneau, E. I. Corwin, G. Parisi, and F. Zamponi, *Phys. Rev. Lett.* **109**, 205501 (2012).
- [27] T. R. Kirkpatrick and P. G. Wolynes, *Phys. Rev. A* **35**, 3072 (1987).
- [28] P. Charbonneau, J. Kurchan, G. Parisi, P. Urbani, and F. Zamponi, [arXiv:1605.03008](#) (2016).
- [29] P. Charbonneau, Y. Jin, G. Parisi, and F. Zamponi, *Proceedings of the National Academy of Sciences* **111**, 15025 (2014).
- [30] M. Skoge, A. Donev, F. H. Stillinger, and S. Torquato, *Physical Review E (Statistical, Nonlinear, and Soft Matter Physics)* **74**, 041127 (pages 11) (2006).
- [31] P. Charbonneau, A. Ikeda, J. A. van Meel, and K. Miyazaki, *Phys. Rev. E* **81**, 040501 (2010).
- [32] C. Rainone, P. Urbani, H. Yoshino, and F. Zamponi, *Physical Review Letters* **114**, 015701 (2015).
- [33] C. Rainone and P. Urbani, *Journal of Statistical Mechanics: Theory and Experiment* **2016**, 053302 (2016).
- [34] G. Brambilla, D. E. Masri, M. Pierno, L. Berthier, L. Cipelletti, G. Petekidis, and A. B. Schofield, *Physical Review Letters* **102**, 085703 (pages 4) (2009).
- [35] T. Grigera and G. Parisi, *Physical Review E* **63**, 45102 (2001).
- [36] S. Singh, M. Ediger, and J. J. de Pablo, *Nature Materials* **12**, 139 (2013).
- [37] L. Berthier, D. Coslovich, A. Ninarello, and M. Ozawa, [arXiv:1511.06182](#) (2015).
- [38] L. Berthier, P. Charbonneau, Y. Jin, G. Parisi, B. Seoane, and F. Zamponi, *Proceedings of the National Academy of Sciences* **113**, 8397 (2016).
- [39] S. F. Swallen, K. L. Kearns, M. K. Mapes, Y. S. Kim, R. J. McMahon, M. D. Ediger, T. Wu, L. Yu, and S. Satija, *Science* **315**, 353 (2007).
- [40] W. Götze, *Journal of Physics: Condensed Matter* **11**, A1 (1999).
- [41] T. Maimbourg, J. Kurchan, and F. Zamponi, *Physical review letters* **116**, 015902 (2016).
- [42] S. Franz and G. Parisi, *Journal de Physique I* **5**, 1401 (1995).
- [43] F. Krzakala and L. Zdeborová, *EPL* **90**, 66002 (2010).
- [44] F. Krzakala and L. Zdeborová, *Journal of Physics: Conference Series* **473**, 12022 (2013).
- [45] M. Mézard, G. Parisi, and M. A. Virasoro, *Spin glass theory and beyond* (World Scientific, Singapore, 1987).
- [46] C. Heussinger and J.-L. Barrat, *Physical review letters* **102**, 218303 (2009).
- [47] C. Heussinger, P. Chaudhuri, and J.-L. Barrat, *Soft matter* **6**, 3050 (2010).
- [48] R. Pastore, M. Pica Ciamarra, and A. Coniglio, *Philosophical Magazine* **91**, 2006 (2011).
- [49] R. Seto, R. Mari, J. F. Morris, and M. M. Denn, *Physical review letters* **111**, 218301 (2013).
- [50] H. Vinutha and S. Sastry, *Nature Physics* **12**, 578 (2016).
- [51] R. Candelier and O. Dauchot, *Physical review letters* **103**, 128001 (2009).
- [52] D. Bi, J. Zhang, B. Chakraborty, and R. Behringer, *Nature* **480**, 355 (2011).
- [53] A. Fall, N. Huang, F. Bertrand, G. Ovarlez, and D. Bonn, *Physical Review Letters* **100**, 018301 (2008).
- [54] P. K. Jaiswal, I. Procaccia, C. Rainone, and M. Singh, *Physical review letters* **116**, 085501 (2016).
- [55] E. Tjhung and L. Berthier, [arXiv:1607.01734](#) (2016).
- [56] Y. Jin and H. Yoshino, [arXiv:16XX.XXXXX](#) (2016).
- [57] S. Franz, G. Parisi, F. Ricci-Tersenghi, and T. Rizzo, *The European Physical Journal E: Soft Matter and Biological Physics* **34**, 1 (2011).
- [58] S. K. Nandi, G. Biroli, and G. Tarjus, *Physical review letters* **116**, 145701 (2016).